

Electronic supporting information for

The cation and anion bonding modes make the difference:
unprecedented layered structure, a tetra(hetero)nuclear and a
tri(hetero)nuclear moiety in thioantimonates(V)

Felix Danker, Tobias A. Engesser, Dario Broich, Christian Näther, and Wolfgang
Bensch*

Table S1: Selected bond lengths (Å) and angles (deg) of $\{[\text{Cu}(\text{cyclam})]_3[\text{SbS}_4]_2\}_n \cdot 20n\text{H}_2\text{O}$ (I).^a

Sb(1)-S(2)	2.3235(13)	Cu(1)-N(2)#3	2.015(2)
Sb(1)-S(1)#1	2.3277(7)	Cu(1)-N(1)	2.022(2)
Sb(1)-S(1)#2	2.3277(7)	Cu(1)-N(1)#3	2.023(2)
Sb(1)-S(1)	2.3278(7)	Cu(1)-S(1)	2.962
S(2)-Sb(1)-S(1)#1	108.346(19)	Cu(1)-S(1)	2.960
S(2)-Sb(1)-S(1)#2	108.346(19)	N(2)-Cu(1)-N(2)#3	180.00(12)
S(1)#1-Sb(1)-S(1)#2	110.573(19)	N(2)-Cu(1)-N(1)	85.37(10)
S(2)-Sb(1)-S(1)	108.35(2)	N(2)#3-Cu(1)-N(1)	94.63(10)
S(1)#1-Sb(1)-S(1)	110.571(19)	N(2)-Cu(1)-N(1)#3	94.63(10)
S(1)#2-Sb(1)-S(1)	110.571(19)	N(2)#3-Cu(1)-N(1)#3	85.37(10)
Cu(1)-N(2)	2.015(2)	N(1)-Cu(1)-N(1)#3	180.0

^aSymmetry transformations used to generate equivalent atoms: #1 -x+y, -x, z; #2 -y, x-y, z; #3 -x+5/3, -y+4/3, -z+4/3.

Table S2: Selected Hydrogen bonds (Å, deg) of $\{[\text{Cu}(\text{cyclam})]_3[\text{SbS}_4]_2\}_n \cdot 20n\text{H}_2\text{O}$ (I).^a

D-H...A	d(D-H)	d(H...A)	d(D...A)	<(DHA)
O(1)-H(2O)...O(3)	0.84	1.96	2.719(4)	150.07
O(2)-H(4O)...O(3)#7	0.84	2.00	2.825(4)	167.26
O(3)-H(5O)...O(2)	0.84	1.92	2.733(4)	162.03
O(3)-H(6O)...O(4)	0.84	1.86	2.675(8)	162.54
O(3)-H(6O)...O(4)#9	0.84	2.29	2.853(8)	124.92
O(3)-H(6O)...O(4)#6	0.84	2.04	2.771(8)	145.63
O(1)-H(1O)...S(1)#7	0.84	2.45	3.271(3)	165.37
O(2)-H(3O)...S(1)#8	0.84	2.42	3.241(3)	164.81
N(2)-H(2)...O(1)	1.00	2.19	3.025(3)	139.43
N(1)-H(1)...S(2)#4	1.00	2.45	3.369(2)	152.60

^aSymmetry transformations used to generate equivalent atoms: #4 -x+2/3, -y+1/3, -z+4/3; #5 -x+y+1, -x+1, z; #6 x-y+2/3, x+1/3, -z+4/3; #7 -y+1, x-y+1, z; #8 y+1/3, x+2/3, -z+7/6; #9 y-1/3, -x+y+1/3, -z+4/3.

Table S3: Selected bond lengths (Å) and angles (deg) of $\{[\text{Zn}(\text{cyclam})]_3[\text{SbS}_4]_2\} \cdot 8\text{H}_2\text{O}$ (**II**).^a

Sb(1)-S(1)	2.3562(9)	N(3)-Zn(1)-N(4)	82.82(12)
Sb(1)-S(2)	2.3213(8)	N(1)-Zn(1)-S(1)	99.81(8)
Sb(1)-S(3)	2.3153(9)	N(2)-Zn(1)-S(1)	104.57(8)
Sb(1)-S(4)	2.3153(9)	N(3)-Zn(1)-S(1)	106.33(8)
S(1)-Sb(1)-S(2)	106.11(3)	N(4)-Zn(1)-S(1)	102.51(8)
S(1)-Sb(1)-S(3)	109.47(3)	S(2)-Zn(2)	2.4580(12)
S(1)-Sb(1)-S(4)	107.36(3)	Zn(2)-N(11)	2.250(4)
S(2)-Sb(1)-S(3)	109.72(3)	Zn(2)-N(11)#1	1.960(4)
S(2)-Sb(1)-S(4)	108.78(3)	Zn(2)-N(12)	2.056(3)
S(3)-Sb(1)-S(4)	115.01(3)	Zn(2)-N(12)#1	2.217(3)
Sb(1)-S(1)-Zn(1)	104.45(3)	N(11)#1-Zn(2)-N(11)	154.41(6)
S(1)-Zn(1)	2.3798(8)	N(11)#1-Zn(2)-N(12)	98.15(13)
Zn(1)-N(1)	2.109(3)	N(11)#1-Zn(2)-N(12)#1	84.25(13)
Zn(1)-N(3)	2.115(3)	N(12)-Zn(2)-N(11)	81.28(12)
Zn(1)-N(2)	2.127(3)	N(12)-Zn(2)-N(12)#1	153.99(5)
Zn(1)-N(4)	2.130(3)	N(12)#1-Zn(2)-N(11)	85.58(12)
N(1)-Zn(1)-N(2)	82.83(13)	N(11)-Zn(2)-S(2)	97.59(9)
N(1)-Zn(1)-N(3)	153.44(11)	N(11)#1-Zn(2)-S(2)	107.31(10)
N(1)-Zn(1)-N(4)	87.08(13)	N(12)-Zn(2)-S(2)	103.50(10)
N(3)-Zn(1)-N(2)	94.91(12)	N(12)#1-Zn(2)-S(2)	100.40(9)

^aSymmetry transformations used to generate equivalent atoms: #1 -x+1, -y+1, -z+2.Table S4: Selected Hydrogen bonds (Å, deg) of $\{[\text{Zn}(\text{cyclam})]_3[\text{SbS}_4]_2\} \cdot 8\text{H}_2\text{O}$ (**II**).^a

D-H...A	d(D-H)	d(H...A)	d(D...A)	<(DHA)
O(1)-H(2O1)...O(5)	0.96	2.04	2.982(9)	165.30
O(2)-H(1O2)...O(3)	0.96	1.84	2.744(9)	156.66
O(3)-H(1O3)...O(4)	0.96	1.90	2.815(9)	157.74
O(4)-H(2O4)...O(1)#5	0.96	1.92	2.803(10)	152.40
N(1)-H(1)...S(2)#2	1.00	2.57	3.408(3)	140.92
N(1)-H(1)...S(4)#2	1.00	2.91	3.651(3)	131.41
N(2)-H(2)...S(4)	1.00	2.44	3.401(3)	160.60
N(3)-H(3)...S(3)	1.00	2.36	3.349(3)	169.79
N(4)-H(4)...S(4)#2	1.00	2.68	3.457(3)	135.03
N(11)-H(11)...S(1)#1	1.00	2.57	3.489(3)	153.36
N(12)-H(12)...S(3)	1.00	2.72	3.659(3)	157.39
O(1)-H(1O1)...S(4)	0.96	2.30	3.176(5)	150.94
O(2)-H(2O2)...S(3)	0.96	2.39	3.338(5)	172.10
O(4)-H(1O4)...S(3)#5	0.96	2.43	3.354(6)	162.39

^aSymmetry transformations used to generate equivalent atoms: #1 -x+1, -y+1, -z+2; #2 x-1/2, -y+3/2, z-1/2; #5 -x+2, -y+1, -z+1.

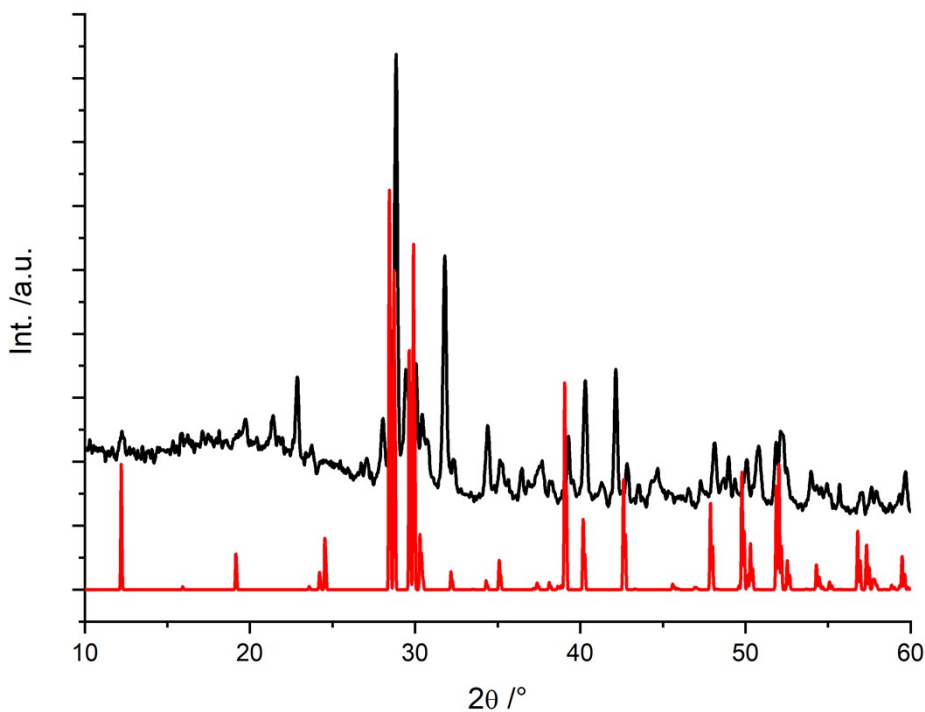


Figure S1: The X-ray powder pattern of the thermal decomposition product of **I** recovered after the TG experiment at $T = 500\text{ }^{\circ}\text{C}$ (black) and the calculated pattern of CuSbS_2 (red).

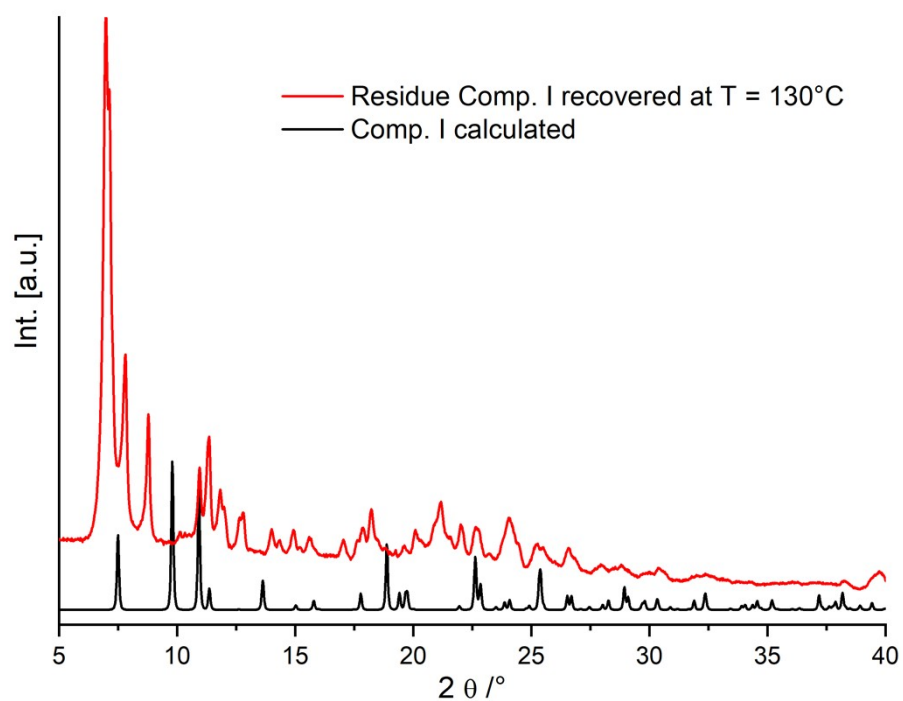
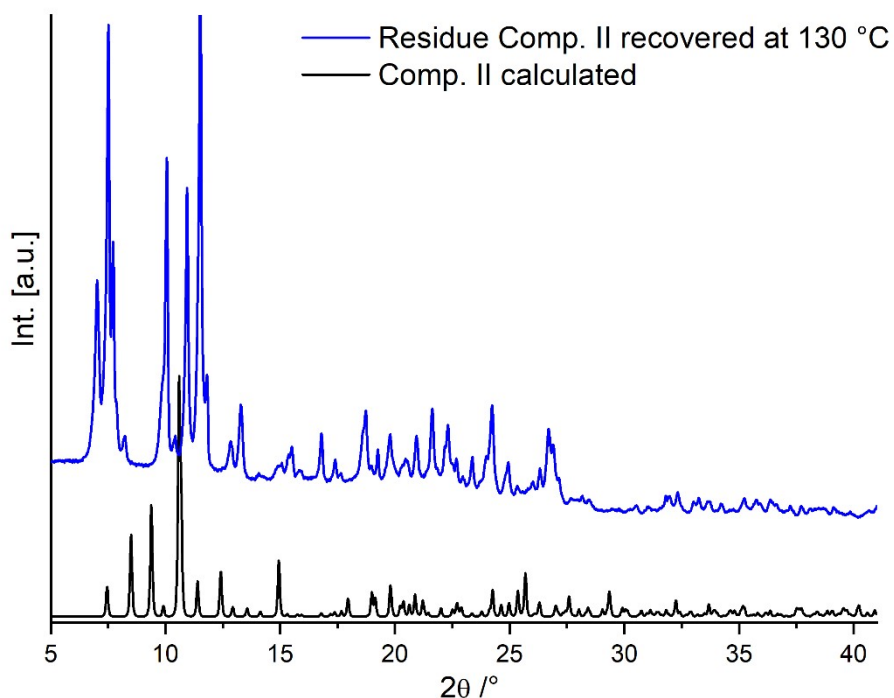
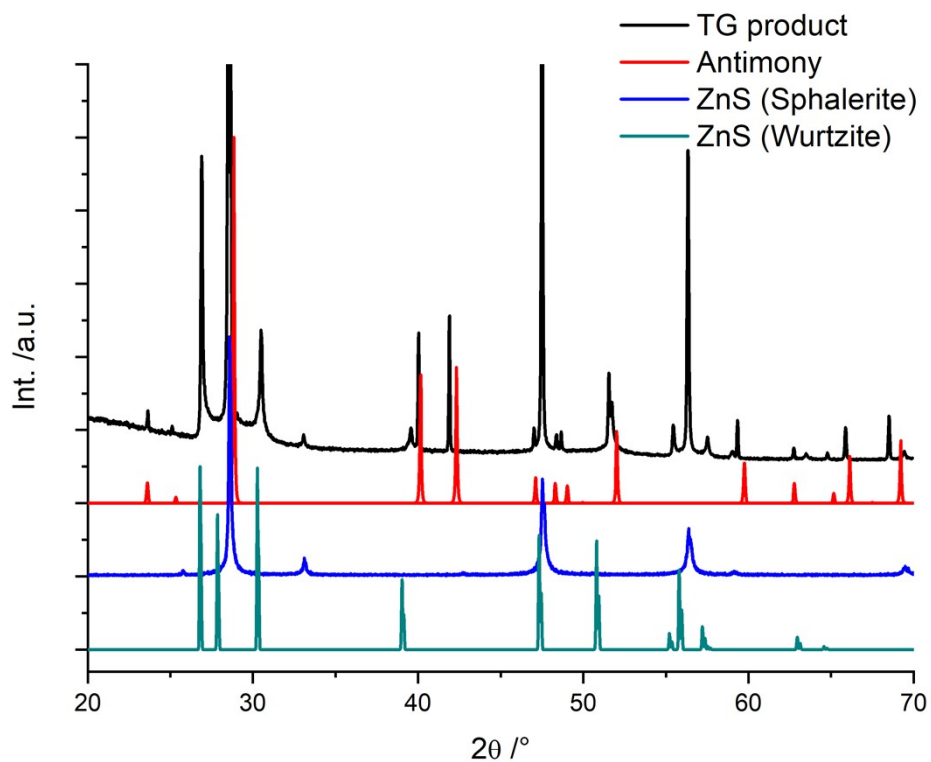


Figure S2: PXRD pattern of the product of the thermogravimetric experiment of compound **I** stopped at $T = 130\text{ }^{\circ}\text{C}$ and the calculated pattern of **I**.



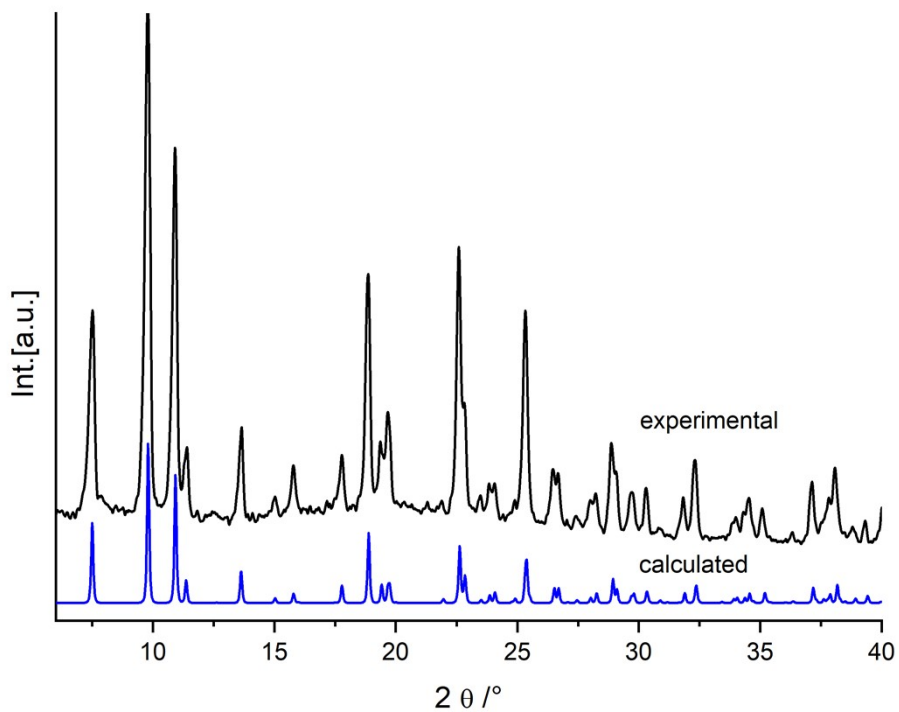


Figure S5: Comparison of the XRD pattern of the reaction product of compound **I** obtained at $T = 130 \text{ } ^\circ\text{C}$ after water uptake with the calculated pattern of **I**.

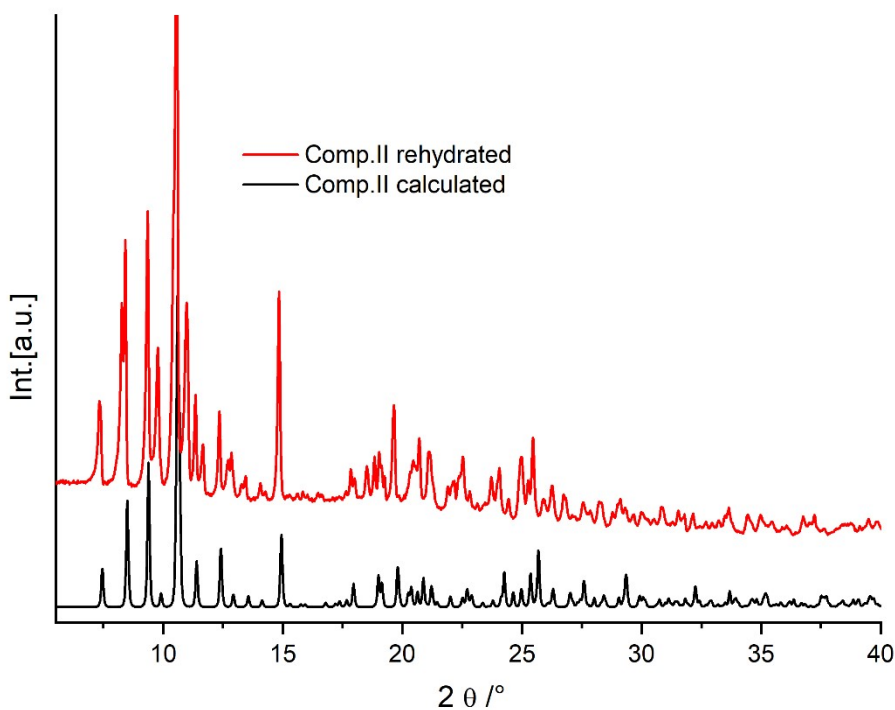


Figure S6: The XRD pattern of the rehydrated product of compound **II** and the calculated pattern for **II**.

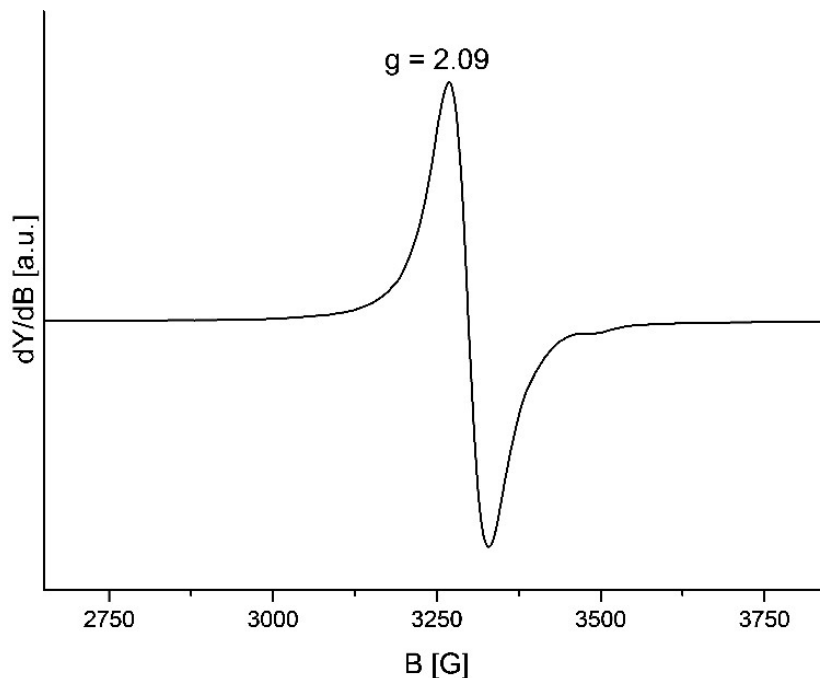


Figure S7: EPR spectrum for compound **I** measured as suspension in a water/glycerine mixture (1:1) at 77 K.

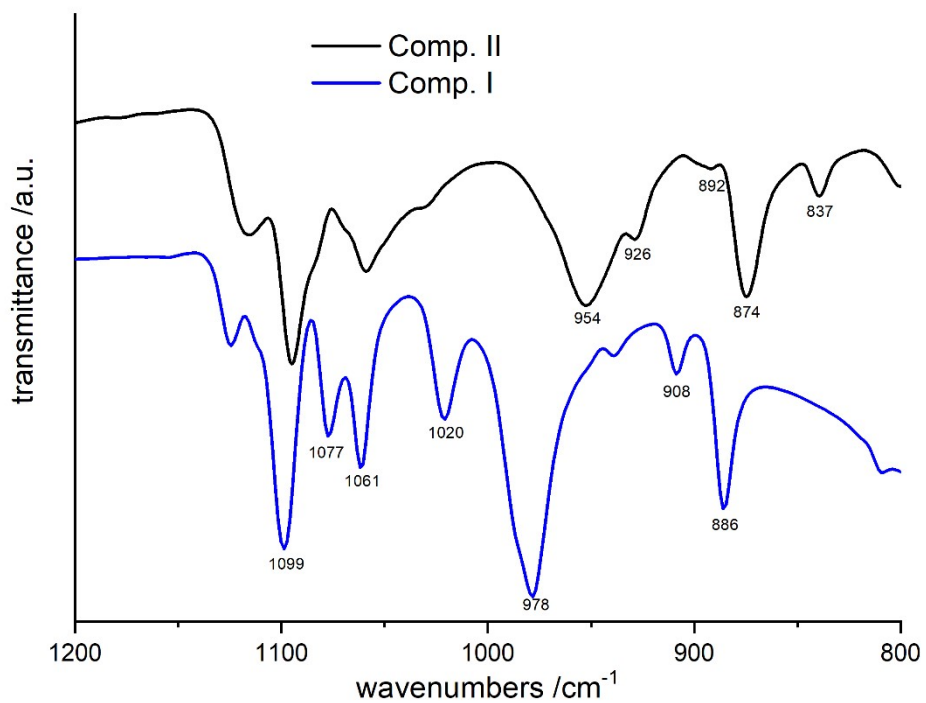


Figure S8: Enlarged view of the IR spectra of compounds **I** and **II**. Some prominent absorptions labeled with the wavenumbers.

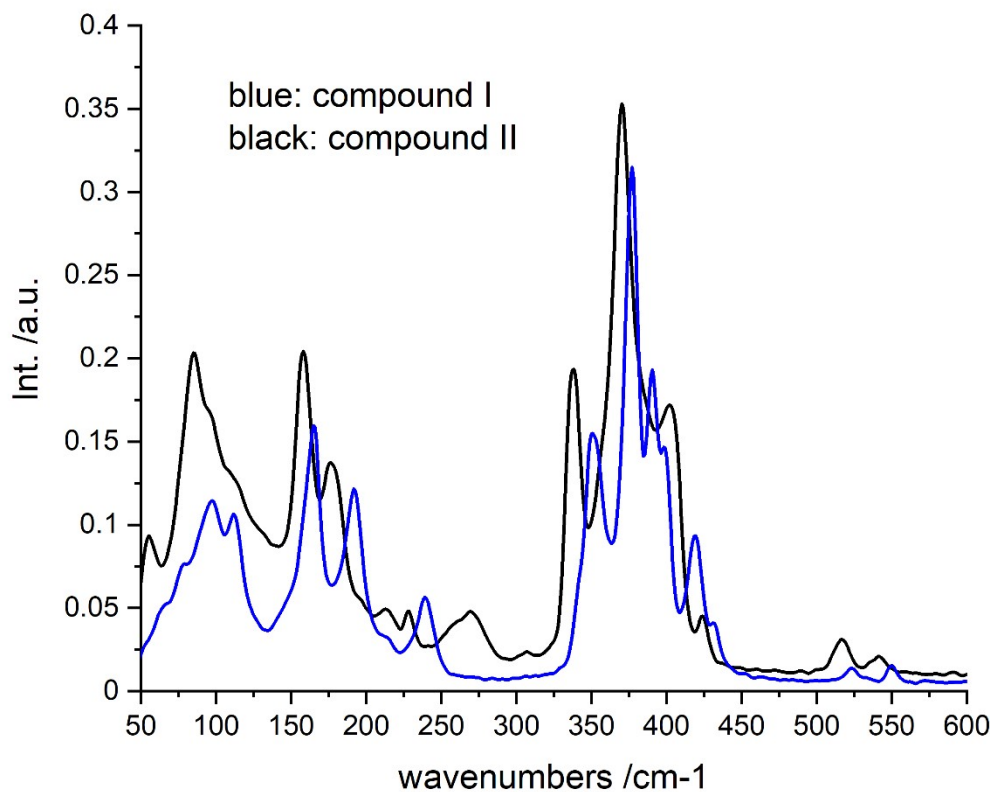


Figure S9: Raman spectra of compounds I and II.

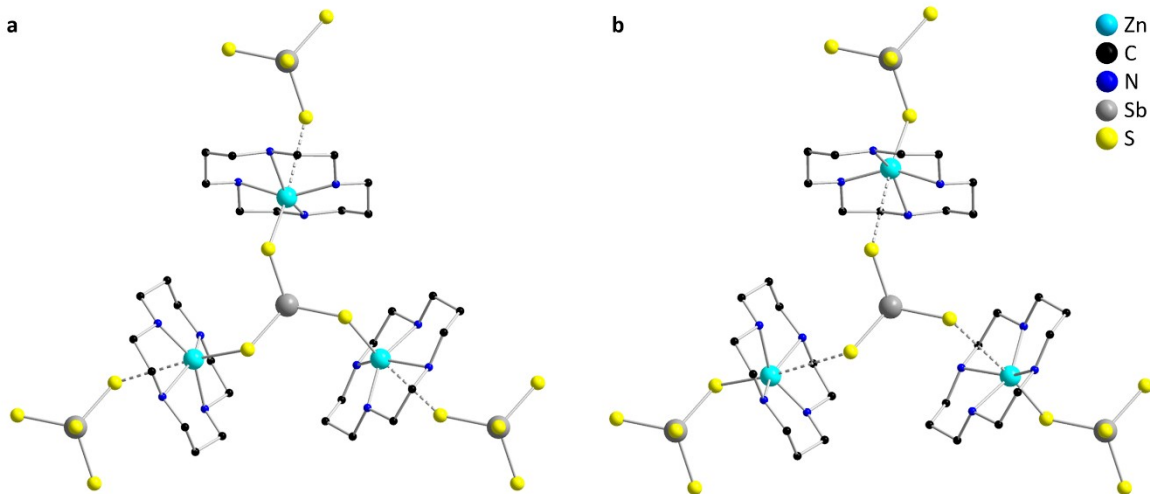


Figure S10: Structures of $[(\text{SbS}_4)\{\text{Zn}(\text{cyclam})\}\text{SbS}_4]_3^{6-}$ fragments used for the simulation of the environment and vibrational frequencies of SbS_4^{3-} at PBE0/def2-SVP level of theory. The effect of the 0.5 occupancy of the Zn1 position in **II** on the coordinating anion is simulated by two versions with “inner” (**a**) and “outer” (**b**) Zn atoms, both exhibiting C_3 symmetry.

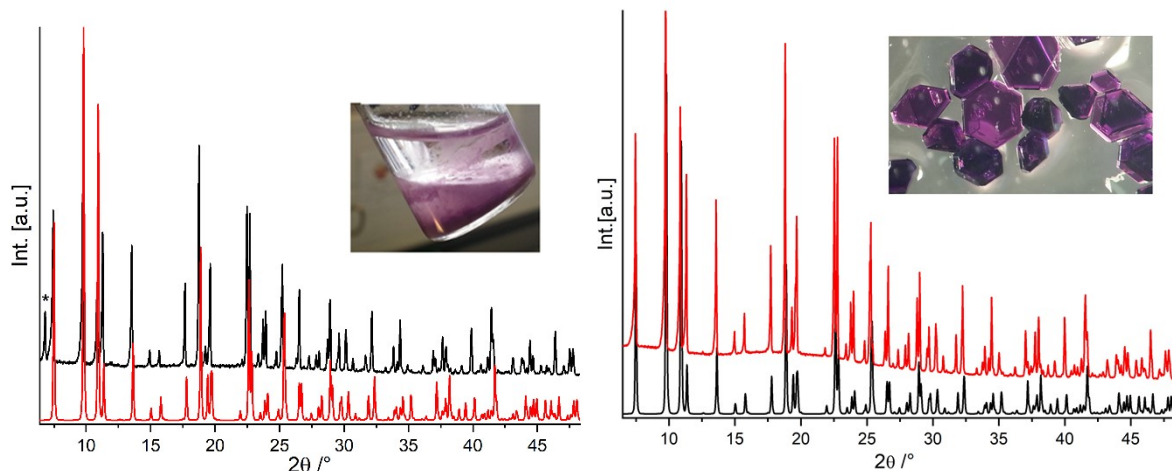


Figure S11: Left: The PXRD pattern of the product filtered after 5 min reaction time (black) and calculated pattern (red) of **I**. The inset shows a photograph of the violet-gray powder; right: the experimental (red) and calculated (black) PXRD patterns of the homogeneous sample. The inset shows a micrograph of the crystals.

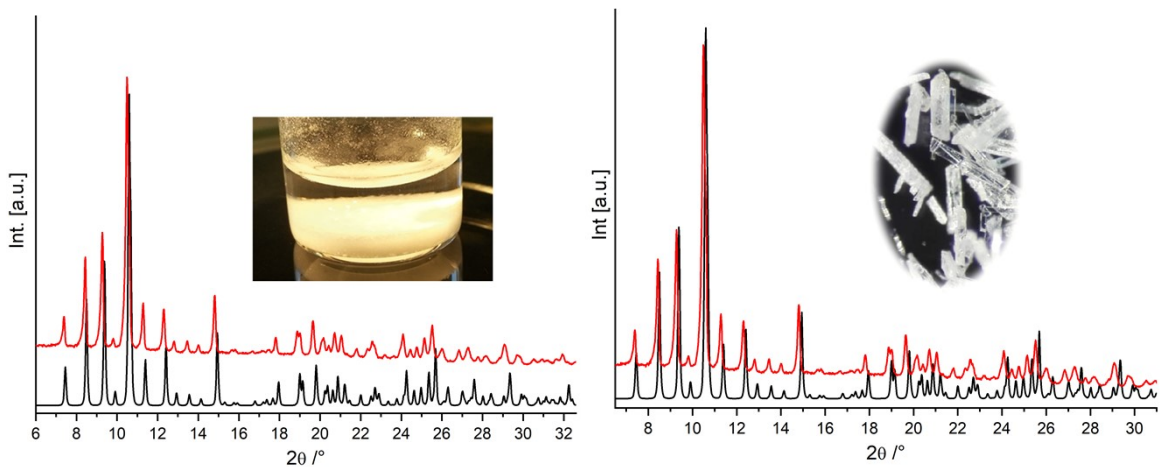


Figure S12: left: PXRD pattern of the solid formed after 5 min. (red) obtained during the synthesis of **II** compared with the pattern of **II** (black). The inset shows a photograph of the colorless precipitate; right: powder pattern of the phase pure sample with the same color code. The inset shows a picture of the crystals.

Computational details

Symmetry considerations

The most favourable symmetry of the $\{[M(\text{cyclam})][\text{SbS}_4]_2\}^{4-}$ complexes ($M = \text{Cu}, \text{Zn}$) in the gas phase was determined by calculations of the corresponding energies on RI-BP86/def2-SVP level and as the structures seem to be highly affected by dispersion also with and without D3(BJ) correction (*Grimme's D3* method with Becke-Johnson damping (BJ)) (Table S5).

Table S5: Absolute and relative (free) energies of $\{[M(\text{cyclam})][\text{SbS}_4]_2\}^{4-}$ complexes ($M = \text{Cu}, \text{Zn}$) in the gas phase with different possible symmetries and with and without dispersion correction (D3(BJ)).

M Symmetry	SCF [Hartree/mol]	SCF [kJ/mol]	H [kJ/mol]	G [kJ/mol]	G_{relative} [kJ/mol]
Cu					
C_1	-5.920,4168	-15.544.048,5105	-15.543.026,6805	-15.543.298,8905	0
C_s^*	-5.920,4032	-15.544.012,5848	-15.542.994,1548	-15.543.260,9448	37,95
C_2^*	-5.920,4032	-15.544.012,5837	-15.542.994,1537	-15.543.260,9337	37,96
C_{2h}^*	-5.920,4032	-15.544.012,5841	-15.542.994,1541	-15.543.259,2341	39,66
<i>D3-BJ corr.</i>					
C_1	-5.920,6053	-15.544.543,1835	-15.543.519,9035	-15.543.786,9835	0
C_s^*	-5.920,5961	-15.544.519,0152	-15.543.499,4152	-15.543.758,5052	28,48
C_2^*	-5.920,5961	-15.544.519,0207	-15.543.499,4307	-15.543.756,8107	30,17
C_{2h}^*	-5.920,5961	-15.544.519,0160	-15.543.499,4260	-15.543.756,8060	30,18
Zn					
C_1	-6.059,2943	-15.908.671,1359	-15.907.647,7059	-15.907.919,8259	0
C_s	-6.059,2943	-15.908.671,1034	-15.907.646,7234	-15.907.915,0434	4,78
<i>D3-BJ corr.</i>					
C_1	-6.059,4802	-15.909.159,1519	-15.908134,3719	-15.908399,3219	0
C_s	-6.059,4802	-15.909.159,0915	-15.908134,2215	-15.908397,2415	2,08

* Symmetry breaking vibrations with imaginary frequencies were found (A'' , B or B_g).

All calculations were performed by using the TURBOMOLE program package.^[1] Structure optimizations were performed at the PBE0^[2]/def2-TZVPP^[3-5] level of theory and with and without Grimme's dispersion correction with Becke-Johnson damping (D3BJ)^[6] as well as the RI approximation^[7] to speed up the calculations. Calculation of vibrational frequencies and to prove that the optimized structure is a minimum on the potential energy surface the AOFORCE module was used,^[8] which is included in the TURBOMOLE program package.

Table S6: Most prominent resonances (cm^{-1}) in the Raman spectra of **I**, and **II** observed in Figure S9.

Compound

I	432	419	398	390	377	351	239	192	165	111
II	424	402	370	337	269	228	213	177	158	

Table S7: Details of the data collection and structure refinement results of compound **I** and **II**.

	$\{[\text{Cu}(\text{cyclam})]_3 [\text{SbS}_4]_2\}_n \cdot 20n\text{H}_2\text{O}$ (I)	$\{[\text{Zn}(\text{cyclam})]_3 [\text{SbS}_4]_2\} \cdot 8 \text{H}_2\text{O}$ (II)
Crystal system	Trigonal	Monoclinic
Space group	$R\bar{3}c$	$P2_1/n$
M (g mol $^{-1}$)	151.91	1439.19
a (Å)	15.5565(4)	10.6285(2)
b (Å)	15.5565(4)	23.7045(5)
c (Å)	48.5419(17)	11.9837(2)
α (°)	90	90
β (°)	90	105.130(2)
γ (°)	120	90
V (Å 3)	10173.5(6)	2914.55(10)
T (K)	170(2)	200(2)
Z	6	2
$D_{\text{calc.}}$ (g cm $^{-3}$)	1.633	1.640
μ (mm $^{-1}$)	2.027	2.468
Scan range (°)	$1.729 < \theta < 27.005$	$1.718 < \theta < 28.001$
Reflections collected	29620	46226
Independent reflections	2478	7024
Min./max. transm.	0.5805/0.8025	0.4640/0.7788
R_{int}	0.0357	0.0373
Reflections with ($I > 2\sigma(I)$)	2270	6224
R values ($I > 2\sigma(I)$)	$R1 = 0.0386$ $wR2 = 0.1005$	$R1 = 0.0412$ $wR2 = 0.1144$
R values (all data)	$R1 = 0.0434$ $wR2 = 0.1042$	$R1 = 0.0466$ $wR2 = 0.1196$
Goodness-of-fit	1.144	1.055

on F^2		
Res. elec. dens. (e Å ⁻³)	0.627 and -0.660	1.133 and -0.746

References

- [1] R. Ahlrichs, M. Bär, M. Häser, H. Horn and C. Kölmel, *Chem. Phys. Lett.*, 1989, **162**, 165; TURBOMOLE v7.2 **2017**, a development of University of Karlsruhe and Forschungszentrum Karlsruhe GmbH, **1989-2007**, TURBOMOLE GmbH, since 2007; available from <http://www.turbomole.com>.
- [2] J. P. Perdew, K. Burke, M. Ernzerhof, *Phys. Rev. Lett.* **1996**, *77*, 3865–3868.
- [3] A. Hellweg, C. Hättig, S. Höfener, W. Klopper, *Theor. Chem. Acc.* **2007**, *117*, 587–597.
- [4] F. Weigend, *Phys. Chem. Chem. Phys.* **2006**, *8*, 1057–1065.
- [5] F. Weigend, R. Ahlrichs, *Phys. Chem. Chem. Phys.* **2005**, *7*, 3297–3305
- [6] a) S. Grimme, J. Antony, S. Ehrlich, H. Krieg, *J. Chem. Phys.* **2010**, *132*, 154104; b) S. Grimme, S. Ehrlich, L. Goerigk, *J. Comput. Chem.* **2011**, *32*, 1456.
- [7] a) K. Eichkorn, H. Treutler, H. Öhm, M. Häser, R. Ahlrichs, *Chem. Phys. Lett.* **1995**, *283*, 240; b) K. Eichkorn, F. Weigend, O. Treutler, R. Ahlrichs, *Theor. Chem. Acc.* **1997**, *97*, 119; c) F. Neese, *J. Comput. Chem.* **2003**, *24*, 1740.
- [8] O. Treutler, R. Ahlrichs, *J. Chem. Phys.* **1995**, *102*, 346.